Original Article

Tumor-derived exosomal miR-103a-3p promotes vascular permeability and proliferation by targeting ZO-1 and ACOX-1 in nasopharyngeal carcinoma

Ying Shan[1,2,3#], Hongmei Fan[4#], Linlin Chai[3,5#], Xiuzhi Kong[3,5], Haijuan Xiao[3,5], Mengdie You[3,5], Yiwen You[1,2,3]^

[1]Suzhou Medical College of Soochow University, Suzhou, China; [2]Department of Otorhinolaryngology Head and Neck Surgery, Affiliated Hospital of Nantong University, Nantong, China; [3]Institute of Otolaryngology Head and Neck Surgery, Affiliated Hospital of Nantong University, Nantong, China; [4]Otolaryngology Head and Neck Surgery, Affiliated Rugao Hospital of Nantong University, Nantong, China; [5]Medical College of Nantong University, Nantong, China

Contributions: (I) Conception and design: Y You; (II) Administrative support: Y You, Y Shan; (III) Provision of study materials or patients: H Fan, L Chai; (IV) Collection and assembly of data: Y Shan, H Fan, L Chai; (V) Data analysis and interpretation: X Kong, H Xiao, M You; (VI) Manuscript writing: All authors; (VII) Final approval of manuscript: All authors.

[#]These authors contributed equally to this work.

Correspondence to: Yiwen You, MD. Suzhou Medical College of Soochow University, 199 Ren'ai Road, Suzhou Industrial Park, Suzhou 215006, China; Department of Otorhinolaryngology Head and Neck Surgery, Affiliated Hospital of Nantong University, Nantong, China; Institute of Otolaryngology Head and Neck Surgery, Affiliated Hospital of Nantong University, Nantong, China. Email: youyiwen_nantong@163.com; youyiwen_ent@163.com.

Background: miR-103a-3p has been reported to be a factor leading to poor prognosis in several human malignancies, including nasopharyngeal carcinoma (NPC). Secreted microRNAs containing exosomes may mediate the communication between cancer and stromal cells. The purpose of the current work was to learn more about miR-103a-3p's function in NPC exosomes.

Methods: Transmission electron microscopy and NanoSight analysis were used to verify the existence of exosomes. To determine the relationship between exosomal miR-103a-3p and carcinogenesis in NPC, gain- and loss-of-function studies were carried out. Cell Counting Kit-8 (CCK8), 5-ethynyl-2'-deoxyuridine (EdU) cell proliferation assay, colony formation, flow cytometry, trans-endothelial invasion assays, endothelial permeability and cellular immunofluorescence were used to identify roles of exosomal miR-103a-3p *in vitro*. Zebrafish assay was used to disclose the effect of exosomal miR-103a-3p *in vivo*. Bioinformatics and dual-luciferase reporter assay were applied to clarify the mechanism of exosomal miR-103a-3p regulating the crosstalk between NPC cells and human umbilical vein endothelial cells (HUVECs).

Results: In the present study, we first demonstrated that the overexpression of exosomal miR-103a-3p improved NPC cell proliferation, migration, and the epithelial-mesenchymal transition (EMT) progression *in vitro*. Then, we verified that NPC cell-derived exosomal miR-103a-3p destroyed the integrity of the endothelial monolayer *in vitro* and *in vivo* by downregulating zonula occludens 1 (ZO-1) expression. Moreover, we revealed that miR-103a-3p containing exosomes facilitated NPC cell proliferation through lipid droplet accumulation by direct target to metabolic enzyme acyl-CoA oxidase 1 (ACOX-1).

Conclusions: Our data demonstrate that exosomal miR-103a-3p can facilitate the development of NPC by regulating the crosstalk between NPC cells and HUVECs. Exosomal miR-103a-3p could potentially serve as a therapeutic target for NPC.

Keywords: Nasopharyngeal carcinoma (NPC); exosomes; miR-103a-3p; zonula occludens 1 (ZO-1); acyl-CoA oxidase 1 (ACOX-1)

^ ORCID: 0000-0002-4171-1621.

Submitted Dec 24, 2023. Accepted for publication Jul 19, 2024. Published online Sep 23, 2024.
doi: 10.21037/tcr-23-2359
View this article at: https://dx.doi.org/10.21037/tcr-23-2359

Introduction

Nasopharyngeal carcinoma (NPC), a frequent malignant neoplasm of the head and neck endangering human health, is caused by the aberrant and uncontrolled development of the nasopharyngeal epithelium (1). The age-standardized incidence rate is 0.5 per 100,000 in Northern Europe, but it increases to 10.2 per 100,000 in places like South-Eastern Asia (2). The combined use of intensity-modulated radiotherapy and magnetic resonance imaging, as well as chemotherapy and advanced radiotherapy, have substantially improved the prognosis of NPC patients (3,4). To create new NPC therapeutics, it is crucial to understand the pathogenesis and metastatic processes.

In a range of cancers, including NPC, microRNAs (miRNAs) serve crucial roles in cell cycle regulation, programmed cell death, cell proliferation, differentiation, cancer initiation, and metastasis (5). Recent research has shown that exosomes play critical roles in regulating tumor-microenvironment cross-talk through the horizontal transfer of miRNAs, messenger RNA (mRNA), and proteins (6). Exosomes are nanoscale packets that vary in size from 40 to 160 nm and are created by the endocytosis, fusion, and exudation of various cells such as cancer cells, human umbilical vein endothelial cells (HUVECs), and mesenchymal stem cell (MSC) (7,8). Exosomes from tumors can transport miRNA and other small molecules to enhance cell-to-cell contact (9). Shen and He showed that MSC-derived exosomes regulate the polarization and inflammatory response of macrophages via miR-21-5p to promote repair after myocardial reperfusion injury (8). More and more research has revealed that tumor-derived exosomes assist in creating a pre-metastatic niche, remodeling the extracellular matrix, promoting epithelial-mesenchymal transition (EMT) and activating mesenchymal stroma cells to support early tumor cell engraftment and metastasis by creating favorable microenvironments (9-11). In preliminary work, our team found that metastasis-associated NPC-derived exosomes containing miR-23a increased angiogenesis by targeting TSGA10 (12). Liu *et al.* showed that exosome-transmitted miR-29a induces colorectal cancer (CRC) metastasis by destroying the vascular endothelial barrier (9).

Metastasis is a complex multistep process involving invasion, intravasation, circulation, extravasation, and seeding into the metastatic site (13). A critical stage in the metastasis process is the escape of malignant cells past the vascular barrier. Increased vascular permeability makes spreading easier (14). The endothelial junction will become less robust and vascular permeability will rise as a result of the depletion of membrane-associated adhesion molecules, harming the vascular barrier and making it simpler for cancer cells to spread throughout the body (15). It has been shown that several miRNAs secreted by tumor cells, including miR638 (16), miR-27b-3p (17) and miR29a (9) control the expression of vascular endothelial cadherin (VE-cadherin) or zonula occludens 1 (ZO-1) to mediate vascular permeability. However, more research is required to determine how vascular permeability is increased by NPC-derived exosomes to control pre-metastatic niche development.

Recent data indicate that the regulation of tumor progression by miRNAs, including tumor proliferation, tumor metastasis, and tumor multidrug resistance, frequently involves dual or multiple targets. Acyl-CoA oxidase 1 (ACOX-1) is the first rate-limiting enzyme in peroxisomal fatty acids beta-oxidation (18). The process in peroxisomes is catalyzed by ACOX, leading to the production of adenosine-triphosphate (ATP) and intermediate products, such as H_2O_2 (19). ACOX-1 was

Highlight box

Key findings

- miR-103a-3p containing exosomes mediated an intercellular communication between nasopharyngeal carcinoma (NPC) cells and blood vessel endothelium by targeting adherent junction protein zonula occludens 1 (ZO-1) and acyl-CoA oxidase 1 (ACOX-1).

What is known and what is new?

- miR-103a-3p increases NPC cell viability, motility, and invasion.
- Exosomal miR-103a-3p facilitates NPC cells metastasis by targeting ZO-1 and causes abnormal lipid metabolism to enhance tumor growth by targeting ACOX-1.

What is the implication, and what should change now?

- Cancer-derived exosomal miR-103a-3p causes vascular leakiness and tumor proliferation, which in turn promotes NPC progression.

observed to induce the degradation of the tumor suppressor p73, resulting in the inhibition of chemotherapy-induced apoptosis in lymphoma cells (20). Multiple independent types of research have suggested the inhibitory role of ACOX-1 in cancer (21). In homozygous ACOX-1 knockout mice, activation of endoplasmic reticulum (ER) stress promoted the development of hepatocarcinogenesis (22). The reduction of ACOX-1, a tumor suppressor, promotes CRC proliferation (21). Lai *et al.* reported that miR-31-5p targets ACOX-1-dependent fatty acid oxidation (FAO), resulting in the intracellular accumulation of lipids which ultimately promotes oral squamous cell carcinoma progression (23). In this study, we identified ACOX-1 as a novel target of miR-103a-3p and showed that it further mediated the proper lipid metabolic profiles.

The current study demonstrated that miR-103a-3p functioned as a tumor-promoting miRNA in NPC and engaged in cell-cell communication via exosomes. miR-103a-3p containing exosomes not only significantly facilitated the migration but also accelerated cell-cycle transition and proliferation of NPC cells. Mechanistic analyses suggested that miR-103a-3p directly targeted ZO-1 and metabolic enzyme ACOX-1. A protocol was prepared before the study without registration. This manuscript is written following MDAR and ARRIVE reporting checklists (available at https://tcr.amegroups.com/article/view/10.21037/tcr-23-2359/rc).

Methods

Cell culture and tissue samples

The normal nasopharynx epithelial cell line NP69 cells were cultured in keratinocyte-SFM (serum-free medium) supplemented with epidermal growth factor (EGF) (Invitrogen, Carlsbad, CA, USA). Human NPC cells CNE2 (low differentiation), CNE1 (high differentiation), 5–8F (high tumorigenesis and high metastasis), 6–10B (low tumorigenesis and low metastasis) cells were cultured in RPMI (Roswell Park Memorial Institute)1640 medium (Biological Industries Israel Beit-Haemek,04–001-1ACS). The cells above were provided as donation by Sun Yat-Sen University and Xiang-Ya School of Medicine. HUVECs were cultured in DMEM (dulbecco's modified eagle medium) /F-12 (HAM)1:1 (Biological Industries Israel Beit-Haemek, 01-19 72-1ACS) containing 10% fetal bovine serum (FBS). 10% fetal bovine serum (Gibco, USA), 0.1% antibiotics for mycoplasma (Invitrogen), and 1% antibiotics (HyClone, USA) were added to the nutritional medium. All cells were multiplied in a natural environment (humidified atmosphere with 5% CO_2, 37 ℃). Tissues samples from pathologically confirmed 7 cases of NPC and 8 cases of normal donors were collected at the Affiliated Hospital of Nantong University following ethics committee approval (IRB No. 2018-L052). Serum samples from NPC patients (n=5) and normal donors (n=5) above were further used. The study was conducted in accordance with the Declaration of Helsinki (as revised in 2013). All included patients had provided informed consent and had not received any cancer therapies prior to biopsy.

Exosomes isolation, identification and miRNA quantitative analysis

NP69 and CNE2 cells were cultured in regular media up to 80% confluence, at which point exosome-depleted medium (10% exosome-depleted FBS) (Life Technologies) was added. Exosomes were harvested by ultra-centrifugation after the conditioned medium (about 50 mL) was collected (24). Briefly, the conditional medium (CM) was centrifuged at 300 ×g for 5 min, 3,000 ×g for 20 min, 6,000 ×g for 40 min, and 10,000 ×g for 60 min to eliminate cell debris, cell fragments and large extracellular vesicles. After that, the pellets were redissolved in phosphate buffered saline (PBS) and the supernatants were centrifuged for 1 hour at 110,000 g and 4 ℃. Prior to use, the pellet was either refrigerated at −80 ℃ or resuspended in particle-free PBS. Transmission electron microscopy (TEM, JEOL, Japan) and NanoSight analysis (NanoSight NS-300 instrument) was used to analyze the morphology and size of exosomes. Exosomes containing microRNA were extracted from CM and plasma using the exoRNeasy Serum/Plasma Starter Kit (QIAGEN) in accordance with the manufacturer's instructions. Utilizing the miRNA First Strand complementary DNA (cDNA) Synthesis Kit (Vazyme Biotech), reverse transcription was performed on 0.5 g of the previously purified total RNA. miR-103a-3p primer (MQPS0000424-1-200) was purchased from Ribobio (Guangdong, China).

Exosome labeling and tracking

Assays for tracking exosomes were carried out as previously mentioned (24). Exosomes were stained for five minutes with PKH67 dye (Sigma, USA), after which they were treated with 1% bovine serum albumin (BSA) solution and then cocultured with cells for 2 hours at 37 ℃. Hoechst

was then used to stain recipient cells, and confocal laser microscopy was used to view the results.

Transfection

CNE2 cells grown to about 70% confluence and then used for cell transfection. Ribobio (Guangdong, China) synthesized the negative control (NC), miR-103a-3p mimic (5'-AGCAGCAUUGUACAGGGCUAUGA-3'), inhibitor (5'-UCAUAGCCCUGUACAAUGCUGCU-3'). Cell transfection was carried out using the Lipofectamine 3000 (Invitrogen). After 48 h of transfection, CNE2 cells and CM were collected for following analysis.

CCK8 (Cell Counting Kit-8) assay

The CCK8 assay was performed using a CCK8 kit following the manufacturer's protocol. Briefly, CNE2 cells were plated into 96-well plates (5×10^3 cells per well) in 100 µL of culture medium and allowed to adhere overnight at 37 ℃. After indicated treatment, CCK-8 solution (100 µL/well) was added for another 1 h. Then, the optical density (OD) was measured with a microplate reader at 450 nm.

EdU (5-ethynyl-2'-deoxyuridine) cell proliferation assay

A cell proliferation experiment was carried out using the Cell-Light Edu Apollo 567 In Vitro Kit (RiboBio). After cell adhesion, 5×10^3 CNE2 cells/well were grown in 96-well plates and given miR-103a-3p exosome treatment as needed. Cells cultured with EdU reagent (1:1,000 dilution) for 2 h the next day. Following a 15-minute fixation with 4% paraformaldehyde 30 minutes of room-temperature incubation with the Click Reaction Mixture away from light is followed by fluorescent microplate detection. Fluorescence microscopes were used for observation and photography. Photoshop software was used to count EdU-positive cells. The EdU labeling rate (%) = [the number of EdU-positive cells/(the number of EdU-positive cells + EdU-negative cells)] × 100%.

Colony formation assay

Six-well plates were planted with 100 cells per well at 37 ℃ and 5% CO_2 of incubation. Fix the colonies after 7–10 days until colony was obviously formed. Then the plate was gently washed and stained with crystal violet for 30 min. Cell colonies were then counted and analysed.

Migration assay

We added 200 µL completed medium containing 5×10^4 CNE2 cells in the upper chamber (diameter =8 µm; Corning, USA) with the treatment of different exosomes. The bottom chambers were filled with complete culture medium. The non-migrated cells on the upper chamber were removed with a cotton swab after 24 hours of incubation, migrated cells were stained with 0.1% crystal violet for 30 minutes, and 5 randomly chosen fields of view were chosen to count.

In vitro endothelial permeability assay

We seeded 1×10^5 HUVECs per well on transwell inserts and cultured in the 24-wells plate. After grown to be confluent, HUVECs were stimulated with or without miR-103a-3p containing exosomes. Then, rhodamine B isothiocyanate-dextran (rhodamine dextran, average MW 70,000; Sigma-Aldrich, Missouri, USA) diluted by 1:40 with complete culture medium was added to the transwell insert. Dextran transit through endothelial monolayers was measured at the appropriate time. The medium of the bottom well was collected. The fluorescence intensity was quantified at 590 nm excitation.

In vivo invasion assay in zebrafish

After being treated with miR-103a-3p mimics and inhibitors, NPC tumor cells were washed twice in PBS and stained for 30 minutes with Dil (V22885; Invitrogen). A microinjection device was used to administer 10 nL of the mixed tumor cells to tg (kdrl: GFP) zebrafish embryos at 48 h postfertilization (hpf). Embryos were seen and photographed using a microscope. All zebrafish were provided by the Animal Experiment Center of Nantong University. All of the experimental procedures were performed in accordance with protocols approved by the Institutional Animal Care and Research Advisory Committee of Nantong University (No. 20180227-005) and in compliance with institutional guidelines for the care and use of animals. *In vivo* experiments, the estimated sample size can effectively detect significant differences between groups.

Western blot

The total protein was extracted from the cells with the Radio Immunoprecipitation Assay (RIPA) reagent

(Beyotime, Shanghai, China) which contains 10 μg/mL phosphatase inhibitor (Beyotime) and 100 μg/mL phenylmethanesulfonyl fluoride (PMSF) (Beyotime). Sodium dodecyl sulfate-polyacrylamide gel electrophoresis (SDS-PAGE) gels were used to separate 20 μg of protein and then transferred to polyvinylidene fluoride (PVDF) membrane (Millipore, Bedford, MA, USA) for western blot analysis. The initial antibodies were applied to the membrane and incubated overnight at 4 ℃: ZO-1 (Abcam, Cambridge, UK; ab96587, 1:500 dilution), ACOX-1 (Abcam, ab184032, 1:500 dilution), E-cadherin (CST, Beverly, USA; 9782, 1:1,000 dilution), N-cadherin (CST, 9782, 1:1,000 dilution), and Vimentin (CST, 9782, 1:1,000 dilution). β-actin were used as controls. The Tris-buffered saline with Tween-20 (TBST) was washed and then incubated with the corresponding secondary antibody for 1 h. After washing, it was developed by enhanced chemiluminescence (ECL). ImageJ software has been used to analyze.

Immunofluorescence assay

Immunofluorescence assay was performed 48 h after CNE2 cells were co-cultured with exosomes. Then cells first were fixed with 4% paraformaldehyde for 30 min and washed with PBS 5 min for 3 times. Then cells were blocked with 10% FBS for 1 h and incubated with E-cadherin antibodies (CST, 9728, 1:200) at 4 ℃ overnight, respectively. The second antibody (goat anti-rabbit IgG) was added and incubated at 37 ℃ for 1 h. After washed with PBS, Hoechst (Beyotime, 33258) stained with the nuclei for 15 min.

Dual-luciferase reporter assay

Using the PmirGLO vector and miR-103a-3p mimic or NC (Shanghai Genechem Co., Ltd., Shanghai, China), the wild-type or mutant 3'UTR of tight junction protein 1 (TJP1) (also known as ZO-1) and ACOX-1 was created into dual-luciferase reporters and co-transfected in CNE2 cells and HUVECs for 48 h. According to the manufacturer's protocol, the dual luciferase reporter assay kit (Beyotime) was used to determine the relative activity of luciferase. The relative firefly luciferase activity was normalized to Renilla luciferase activity.

Statistical analysis

Each experiment was performed for more than three times. The medium standard deviation was used to express the quantitative data. Student's *t*-test was used to compare the statistical differences between the two groups, and analysis of variance (ANOVA) was used to compare the differences between several groups. To examine overall survival (OS), the Kaplan-Meier technique and log-rank test were applied. A value of $P<0.05$ was considered statistically significant.

Results

miR-103a-3p is upregulated in human NPC tissue and exosomes samples

Based on either unpaired (*Figure 1A*) or paired (*Figure 1B*) analysis, The Cancer Genome Atlas (TCGA) head and neck squamous cell carcinoma (HNSC) cohort analysis revealed that miR-103a-3p was highly increased. Violin plot also showed miR-103a-3p level was significantly higher in HNSC (*Figure 1C*). According to a Kaplan-Meier analysis of the TCGA data, patients with HNSC who had higher miR-103a-3p expression had worse OS than patients who had lower miR-103a-3p expression (*Figure 1D*). miR-103a-3p was significantly elevated in NPC tissues, according to reverse transcription quantitative polymerase chain reaction (RT-qPCR) analyses of fresh NPC tissues (*Figure 1E*). Furthermore, when compared to the immortalized normal human nasopharynx epithelial cell line NP69, cellular miR-103a-3p was found at significantly high levels in NPC cell lines (CNE1, CNE2, 5-8F, and 6-10B). CNE2 had the greatest level of miR-103a-3p expression among the NPC cells (*Figure 1F*). Therefore, CNE2 cells were chosen for the following research.

Previously, miR-103a-3p increased NPC cell viability, motility, and invasion, as shown by Zhao *et al.* (25). We then looked further into the expression of miR-103a-3p in NPC exosomes, because exosomes play a role in the progression and metastasis of cancer by transferring bioactive molecules between cancer and different cells in the local and distant microenvironments (26). Another reason was that miRNA has the potential to be transferred from cell to cell via exosomes (27). First, as our previously published protocol, exosomes were isolated from the CM and characterized by electron microscopy (*Figure 1G*) and NanoSight analysis (*Figure 1H*) to determine the shape and size. The diameter spread of exosomes was consistent with a normal distribution (*Figure 1H*). miR-103a-3p was clearly elevated in exosomes isolated from NPC patients' serum (*Figure 1I*) and the CM of CNE2 cells (*Figure 1J*) in comparison to normal control. We came to the conclusion

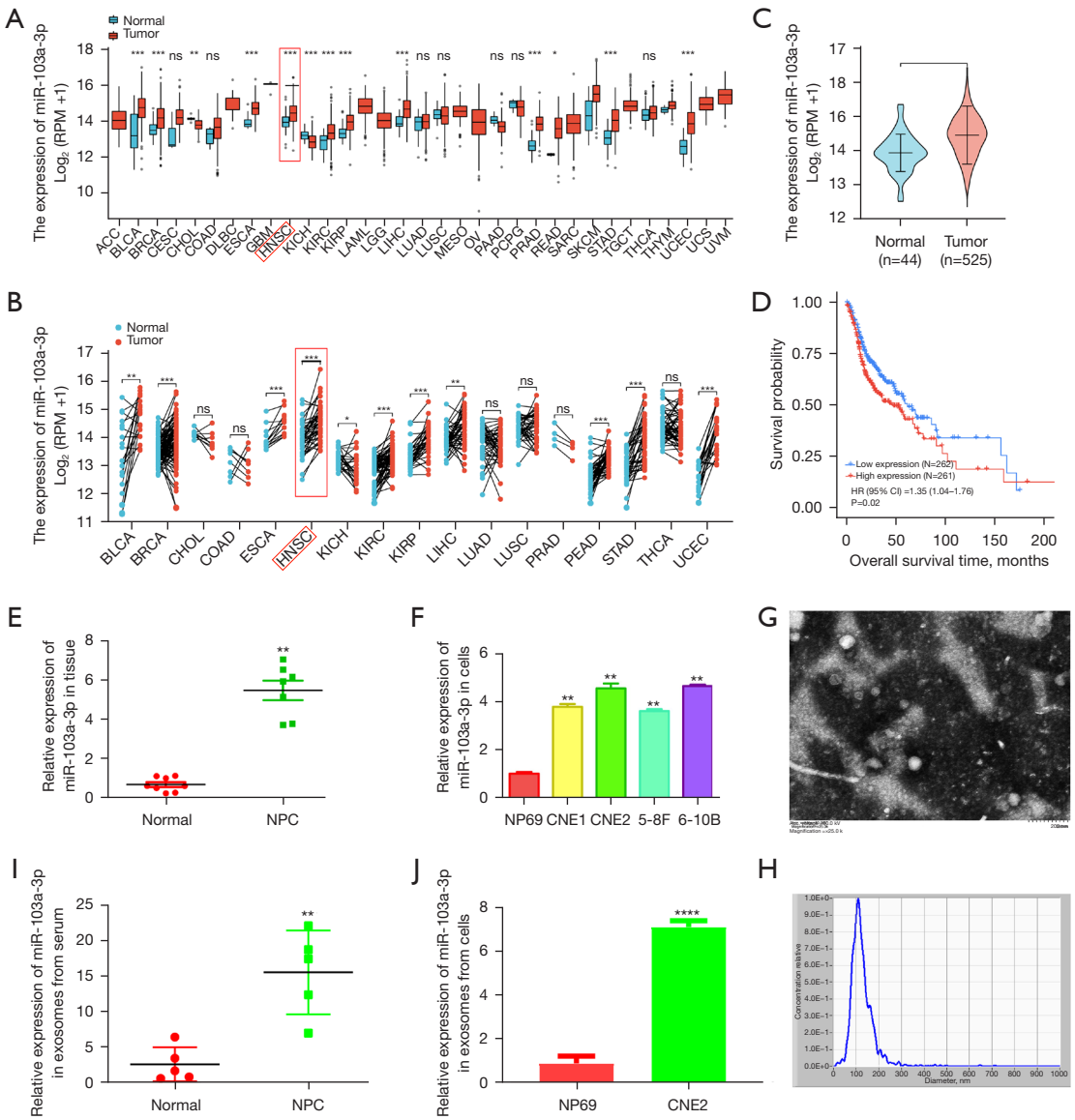

Figure 1 miR-103a-3p is upregulated in human NPC tissue and exosomes samples. (A) miR-103a-3p expression in pan-cancer and normal samples in TCGA. (B) miR-103a-3p expression in matched cancer and normal samples in TCGA. (C) miR-103a-3p expression in the TCGA HNSC cohort. (D) The relationship between miR-103a-3p and OS in HNSC patients was examined using Kaplan-Meier survival analysis. HR: the ratio of two risk rates. HR (95% CI) =1.35 (1.04-1.76) (HR >1), it means that the experimental group (study subjects) is a risk factor relative to the control group. P=0.02. (E,F) RT-qPCR assay was performed to explore the miR-103a-3p expression in human NPC tissues (E) and cells (F) compared to normal controls. (G,H) Exosomes taken from NPC patients' serum were analyzed for phenotypes using electron microscopy at ×25.0 K magnification (G) as well as Nano Sight nanoparticle tracking analysis (H). (I,J) RT-qPCR analysis of the miR-103a-3p expression levels in exosomes which was generated from serum (I) and the conditioned medium (CM) of CNE2 cells (J). Data represent at least three experiments performed in triplicate, ****, P<0.001; ***, 0.001<P<0.01; **, P<0.01; *, P<0.05; ns, non-significant, P>0.05. RPM, reads per million mapped reads; NPC, nasopharyngeal carcinoma; TCGA, The Cancer Genome Atlas; HNSC, head and neck squamous cell carcinoma; OS, overall survival; HR, hazard ratio; CI, confidence interval; RT-qPCR, reverse transcription quantitative polymerase chain reaction.

that exosomal miR-103a-3p might have cancer-promoting effects in NPC and then investigated miR-103a-3p's impact on the development of NPC.

Exosomal miR-103a-3p promotes CNE2 cells migration in vitro and in vivo

Gain and loss of function assays were conducted to look into the function of miR-103a-3p in exosomes using a specific miR-103a-3p mimic and inhibitor. The consistent and high efficiency of miR-103a-3p oligonucleotide transfection was demonstrated by the identical and intense fluorescence seen in miR-103a-3p mimic and inhibitor transfected CNE2 cells (*Figure 2A*). Exosomes isolated from the CM of CNE2 cells transfected with miR-103a-3p mimic revealed a more than 2-fold increase in miR-103a-3p expression when compared to control cells (*Figure 2B*). The miR-103a-3p inhibitor eliminates endogenous miR-103a-3p in CNE2 cells (*Figure 2B*). Exosomal miR103a-3p expression was also assessed by RT-qPCR, as shown in *Figure 2C*, where miR103a-3p oligonucleotides specifically increased or inhibited miR103a-3p expression in exosomes from CNE2 cells. miR-103a-3p was up-regulated in CNE2 cells exposed to exosomes containing overexpressed miR-103a-3p (*Figure 2D*). Exosomes from transfected CNE2 cells were co-cultured with CNE2 cells to see if exosomal miR-103a-3p induces the creation of the pre-metastatic niche. Transwell experiments were used to investigate the regulatory role of exosomal miR-103a-3p on cell migration *in vitro*. The amount of migrating CNE2 cells was larger following culture with exosomes from miR-103a-3p mimic-transfected CNE2 cells than after culture with exosomes from miR-103a-3p inhibitor-transfected CNE2 cells (*Figure 2E,2F*). This conclusion was further confirmed by conducting the zebrafish model *in vivo* (*Figure 2G-2I*). Exosomes isolated from CNE2 cells transfected with miR-103a-3p mimic and inhibitor were combined with Dil-labeled CNE2 cells. The cells were then injected into the zebrafish embryos' yolk sac (*Figure 2G*). The injection of exosomes from the miR103a-3p mimic groups clearly resulted in a faster migration rate of CNE2 cells. In contrast, miR-103a-3p inhibitor groups showed a slowdown in the rate of migrating cells (*Figure 2H,2I*).

Tumor cell migration is often associated with the occurrence of the progression of EMT (28). Then the effect of exosomal miR-103a-3p on EMT of NPC cells was further explored. We found that the EMT construction was verified by the observation of EMT-like cell morphology (a spindle-shaped and fibroblast-like morphology) after co-cultured with miR-103a-3p overexpressed exosomes (Figure S1A). The Western blot assay results showed that miR-103a-3p overexpressed exosomes increased the expression levels of N-cadherin and Vimentin proteins, while decreased the expression level of E-cadherin protein in CNE2 cells, whereas miR-103a-3p down-regulated exosomes led to the opposite results (Figure S1B). Cellular immunofluorescence data also confirmed the result above (Figure S1C). These findings further approve the stimulation of exosomal miR-103a-3p on NCP cells metastasis by EMT.

NPC-secreted exosomal miR-103a-3p promotes proliferation of NPC cells

Then, to confirm whether exosomal miR-103a-3p stimulates NPC cell proliferation, we carried out a number of experiments. CCK8 data showed that, as compared to NC-exosomes, miR-103a-3p overexpressed exosomes improved CNE2 cell proliferation after co-culture (*Figure 3A*). Data of colony formation assays also revealed that cells co-cultured with miR-103a-3p mimic exosomes formed more and larger colonies than NC (*Figure 3B,3C*). miR-103a-3p down-regulated exosomes conspicuously reduced the incorporation of EdU in CNE2 cells (*Figure 3D,3E*). Flow cytometry was used to detect the proportion of cells in the G1, S, and G2 phases, while CNE2 cells were treated with miR-103a-3p mimic or inhibitor exosomes (*Figure 3F*). Results suggested that exosomes contained more miR-103a-3p induced the accumulation of the G2/M-population (*Figure 3F-3H*), indicating that miR-103a-3p facilitated the S-G2/M transition. Taken together, the data above demonstrated that exosomal miR-103a-3p encouraged CNE2 cells to proliferate *in vitro*.

Exosomal miR-103a-3p increases the establishment of pre-metastatic niche by increasing the vascular permeability

Using miRDB, starBase and TargetScan databases, putative targets of miR-103a-3p were identified (*Figure 4A*). Among the predicted targets, tight junction protein 1 (TJP1) and ACOX-1 which are critical in sustaining endothelial cell-cell interactions and proliferation. TJP1 and ACOX-1 were chosen for further validation. The TJP1, also known as zona occludens 1 (ZO-1), was associated with adherence molecules, signaling pathways, and cell-cell junctions, according to an analysis of gene ontology and the Kyoto Encyclopedia of Genes and Genomes (*Figure 4B,4C*). The color of the dots corresponded to the range of the

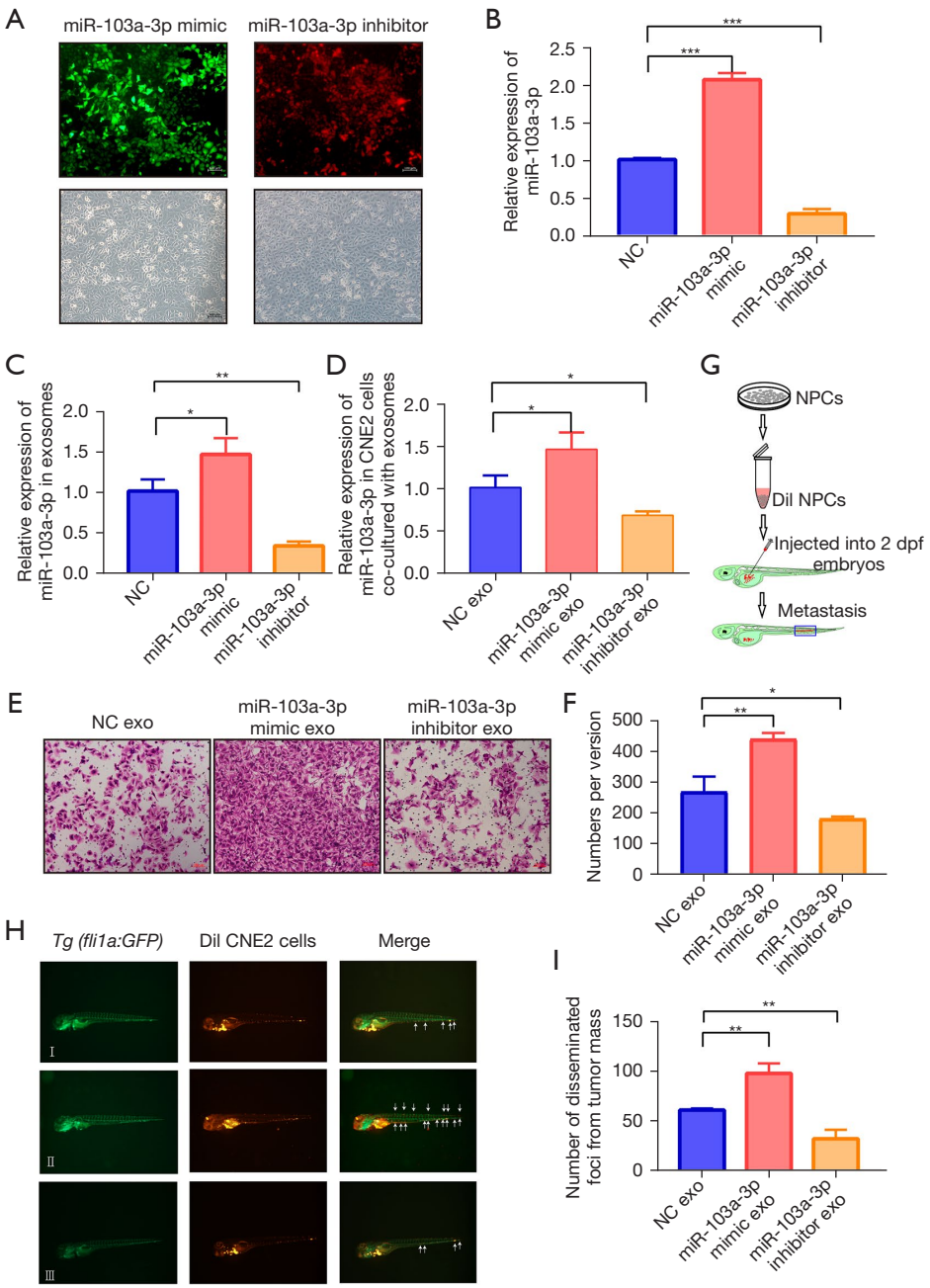

Figure 2 Exosomal miR-103a-3p promotes CNE2 cells migration *in vitro* and *in vivo*. (A) Representative images for fluorescence in miR-103a-3p mimic (green) and a specific inhibitor (red) transfected CNE2 cells. (B,C) RT-qPCR analysis of miR-103a-3p expression levels in transfected CNE2 cells (B) and exosomes (C). (D) RT-qPCR analysis for miR-103a-3p expression in CNE2 cells incubated with exosomes derived from miR-103a-3p mimic and inhibitor transfected cells. (E,F) Crystal violet staining of transwell assays and statistical analysis of CNE2 cells treated with exosomes with different miR-103a-3p level. (G) Schematic diagram of injection in zebrafish. (H,I) Dil-labeled CNE2 cells mixed with exosomes were injected into the zebrafish perivitelline space of 48 hpf (hours post fertilization) embryos. At day 8 post injection, CNE2 cells dissemination was observed using fluorescence microscopy. Arrows indicate tumor foci. Scale bar, 500 nm. Data represent at least three experiments performed in triplicate, *, 0.01≤P<0.05; **, P<0.01; ***, P<0.001. RT-qPCR, reverse transcription quantitative polymerase chain reaction; NC, normal control; NPCs, nasopharyngeal carcinoma cells.

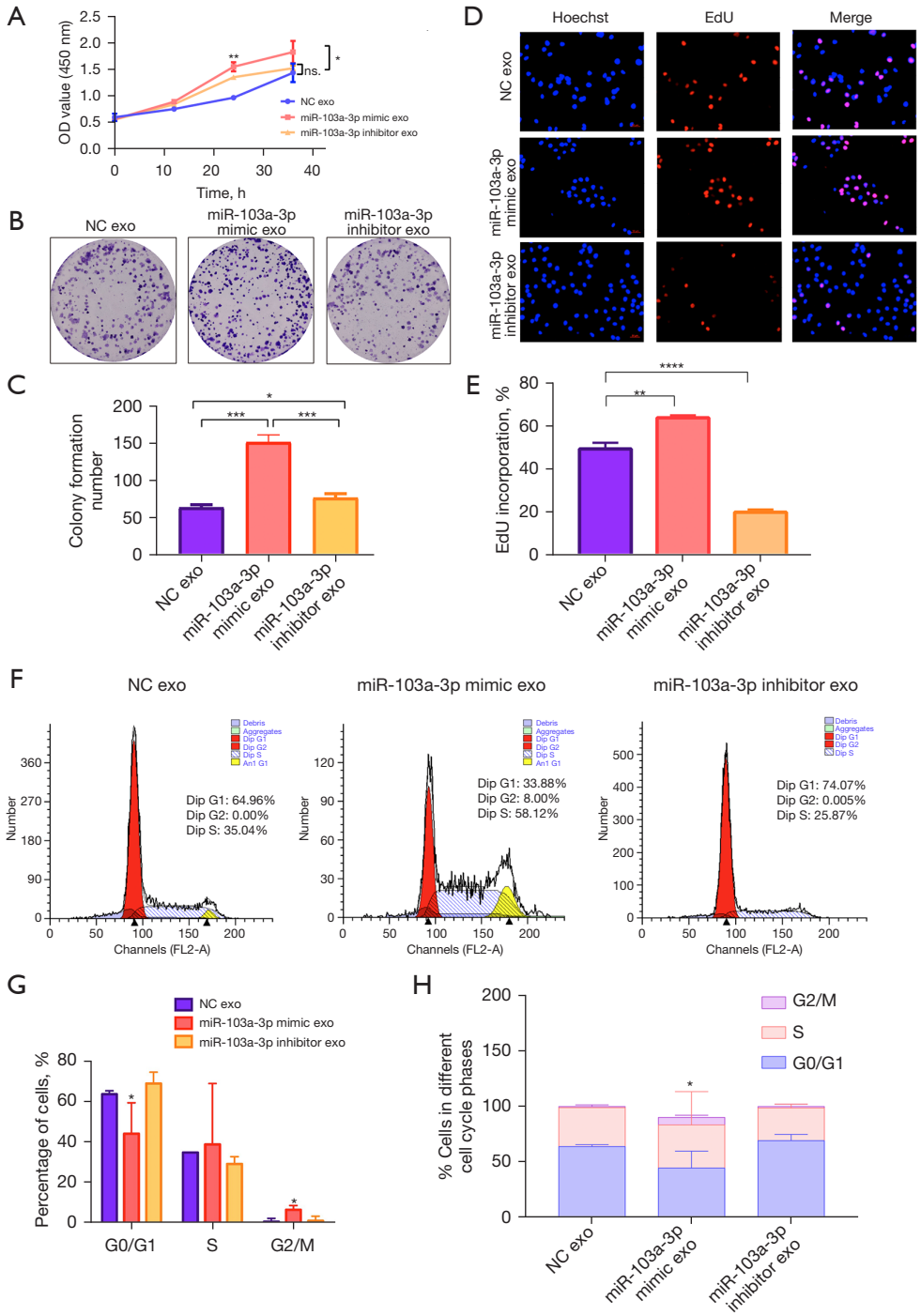

Figure 3 NPC-secreted exosomal miR-103a-3p primes proliferation of NPC cells. (A) Cell viability of different CNE2 cells treated with different exosomes. (B,C) Colony formation capacities in exosomes-cultured CNE2 cells were assessed by crystal violet staining quantification. (D,E) EdU assay was used to analyze the effect of miR-103a-3p mimic or inhibitor-transfected exosomes on CNE2 cell proliferation ability. Representative fluorescence images of EdU staining, nuclei: Hoechst (blue), and proliferating cell: EdU + (red). Magnification: ×20. (F-H) After co-cultured with exosomes, flow cytometry examined cell distribution (%) in different cell cycle phases. Data represent at least three experiments performed in triplicate, ****, P<0.0001; ***, P<0.001; **, P<0.01; *, P<0.05; ns, non-significant. OD, optical density; NPC, nasopharyngeal carcinoma; EdU, 5-ethynyl-2'-deoxyuridine.

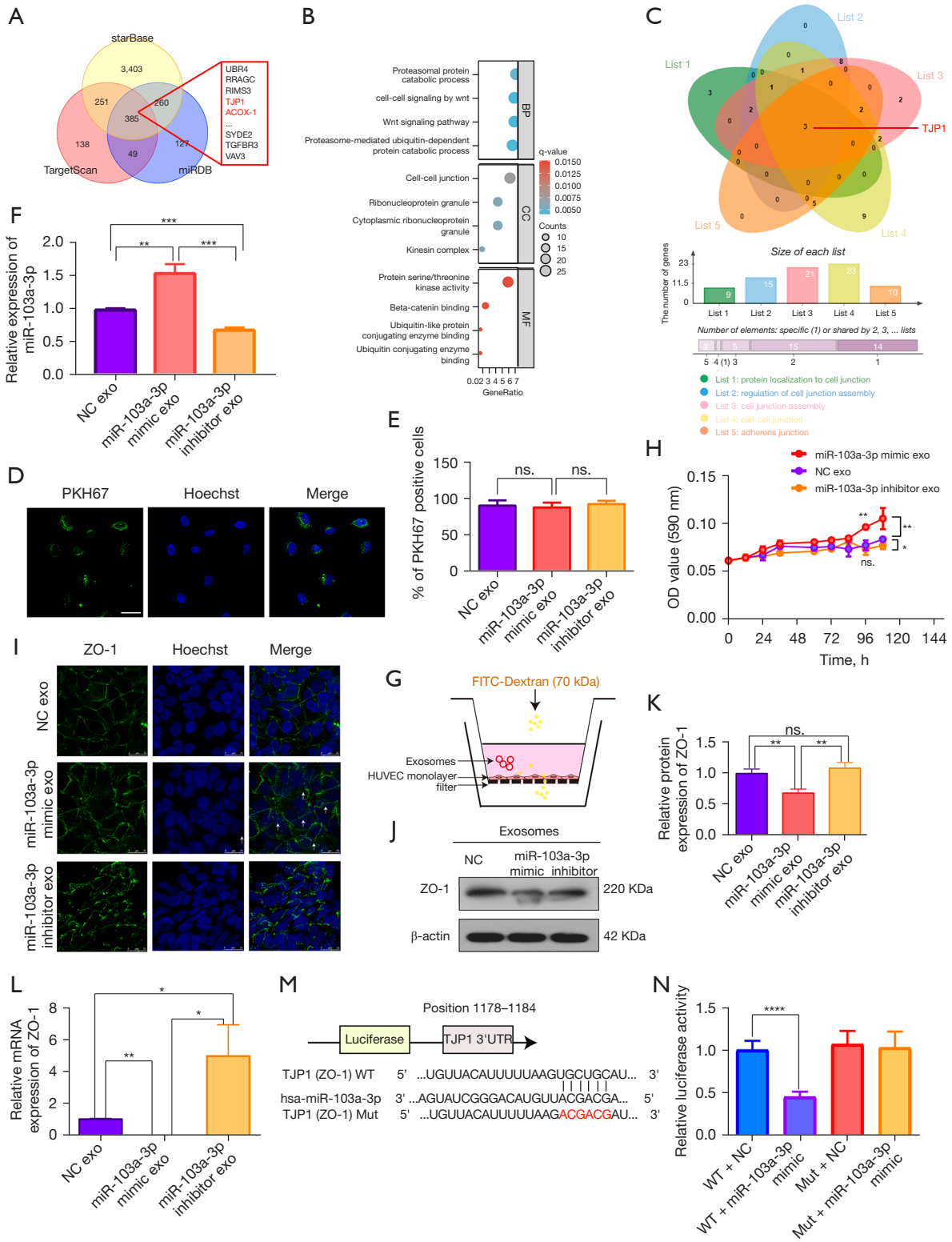

Figure 4 Exosomal miR-103a-3p increases the establishment of pre-metastatic niche by increasing the vascular permeability. (A) miRDB, starBase and TargetScan were used to estimate the potential targets of miR-103a-3p. (B) Scatter plot of pathways enrichment of miR-103a-3p targets. The color of the dots corresponded to the range of the q-value, and the size of the dots indicates the number of genes.

(C) Venn diagram of the differentiated pathways. (D) Confocal microscopy was used to observe that PKH67-labeled (green fluorescence) CNE2 exosomes were taken up by Hoechst stained HUVECs (blue fluorescence). Scale bar =25 μm. (E) Quantification of exosomes which were uptaked by HUVECs. (F) Recipient HUVECs co-cultured with exosomes were examined for miR-103a-3p expression using RT-qPCR. (G) Pattern diagram of *in vitro* permeability experiment. (H) Exosomes from miR-103a-3p mimic or inhibitor transfected cells were incubated with HUVECs before rhodamine-dextran was added to the top chamber and the presence of dextran (OD 590 nm) in the bottom chamber was detected at the specified time. (I) Immunocytochemistry of ZO-1 for HUVECs. Arrow indicated the integrity damage of tight connection. Scale bars, 25 μm. (J,K) ZO-1 protein expression was detected in CNE2 derived exosomes co-cultured with HUVECs using the western blot assay. (L) ZO-1 mRNA expression was analyzed in CNE2 derived exosomes treated HUVECs through RT-qPCR. (M) The 3'UTR of ZO-1's probable miR-103a-3p binding sequence. (N) The relative luciferase activity of the reporter plasmid carrying wild-type, mutant ZO-1 3'-UTR was detected. Data represent at least three experiments performed in triplicate, ****, P<0.0001; ***, P<0.001; **, P<0.01; *, P<0.05; ns, non-significant. BP, biological processes; CC, cellular components; MF, molecular functions; HUVECs, human umbilical vein endothelial cells; OD, optical density; NC, normal control; ZO-1, zonula occludens 1; mRNA, messenger RNA; RT-qPCR, reverse transcription quantitative polymerase chain reaction.

q-value. As we have previously reported the disruption of tight junctions in recipient HUVECs caused by NPC cells secreted exosomes increased vascular permeability and might contribute to metastases (24). To investigate the influence of exosomal miR-103a-3p on the integrity of the endothelial adhesion junction, HUVECs were treated with PKH67-labeled exosomes from CNE2 cells transfected with miR-103a-3p mimic or inhibitor (*Figure 4D*). Incubated HUVECs contained PKH67 lipid dye, and there was no difference between any of the groups (*Figure 4E*). We also discovered the presence of miR-103a-3p in exosomes treated HUVECs. In HUVECs incubated with miR-103a-3p overexpressed exosomes, the RT-qPCR test revealed that miR-103a-3p was up-regulated (*Figure 4F*). We subsequently carried out the *in vitro* permeability assay to assess the passage of rhodamine-labeled dextran across the monolayer of HUVECs pre-treated with the relevant exosomes with the goal to research the influence of exosomal miR-103a-3p on vascular permeability (*Figure 4G*). Pre-treating CNE2 cells with miR-103a-3p mimic exosomes significantly enhanced the amount of dextran that could pass through a HUVEC monolayer compared to control, indicating increased endothelial permeability (*Figure 4H*). On the contrary, the enhancement of vascular permeability was partially reversed by miR-103a-3p inhibited exosomes (*Figure 4H*). Images of immunofluorescence, as showed in *Figure 4I*, miR-103a-3p mimic exosomes disrupted the endothelial cell-cell boundaries indicating loss of contact between endothelial cells. Exosomes from miR-103a-3p mimic-transfected CNE2 cells, caused a reduction in ZO-1 expression in both protein (*Figure 4J*,*4K*) and RNA (*Figure 4L*) level, but not from miR-103a-3p inhibitor-transfected group. The hypothesized relationship between miR-103a-3p and ZO-1 was also verified using a luciferase experiment. The 3'-UTR of ZO-1 contains putative miR-103a-3p binding sites (*Figure 4M*). To confirm that miR-103a-3p directly targets ZO-1, we created mutant and wild-type binding sites and used a luciferase reporter gene assay (*Figure 4N*). This evidence suggests that exosomal miR-103a-3p generated from CNE2 cells affected the integrity of endothelial barriers and increased vascular permeability by directly target ZO-1 which may function as a potential mechanism of metastasis promotion.

Exosomal miR-103a-3p causes abnormal lipid metabolism and enhances tumor growth by targeting ACOX-1 in NPC

An earlier study revealed that lipid droplets which are important promoters of cancer growth, store fatty acids and cholesterol (29). Lipid droplets were stained with BODIPY to further investigate whether miR-103a-3p facelifted NPC cell growth through lipid droplet accumulation. We discovered that while miR-103a-3p mimic treated exosomes co-cultured with CNE2 cells promote an increase in lipid droplet area, miR-103a-3p inhibitor induces the aggregation of small lipid droplets instead (*Figure 5A*,*5B*). Among many putative targets (*Figure 4A*), because of its suppressing role in cell proliferation, ACOX-1 is of particular interest. ACOX-1 was highly increased in head and neck normal tissues, according to TCGA nasopharyngeal cancer cohort analysis (*Figure 5C*). Western blot study of CNE2 cells after treatment with exosomes derived from miR-103a-3p overexpressing cells revealed that ACOX-1 protein expression levels were significantly lower than in control cells (*Figure 5D*,*5E*). In line with the aforementioned findings, recipient CNE2 cells treated with exosomes from CNE2 cells with high miR-103a-

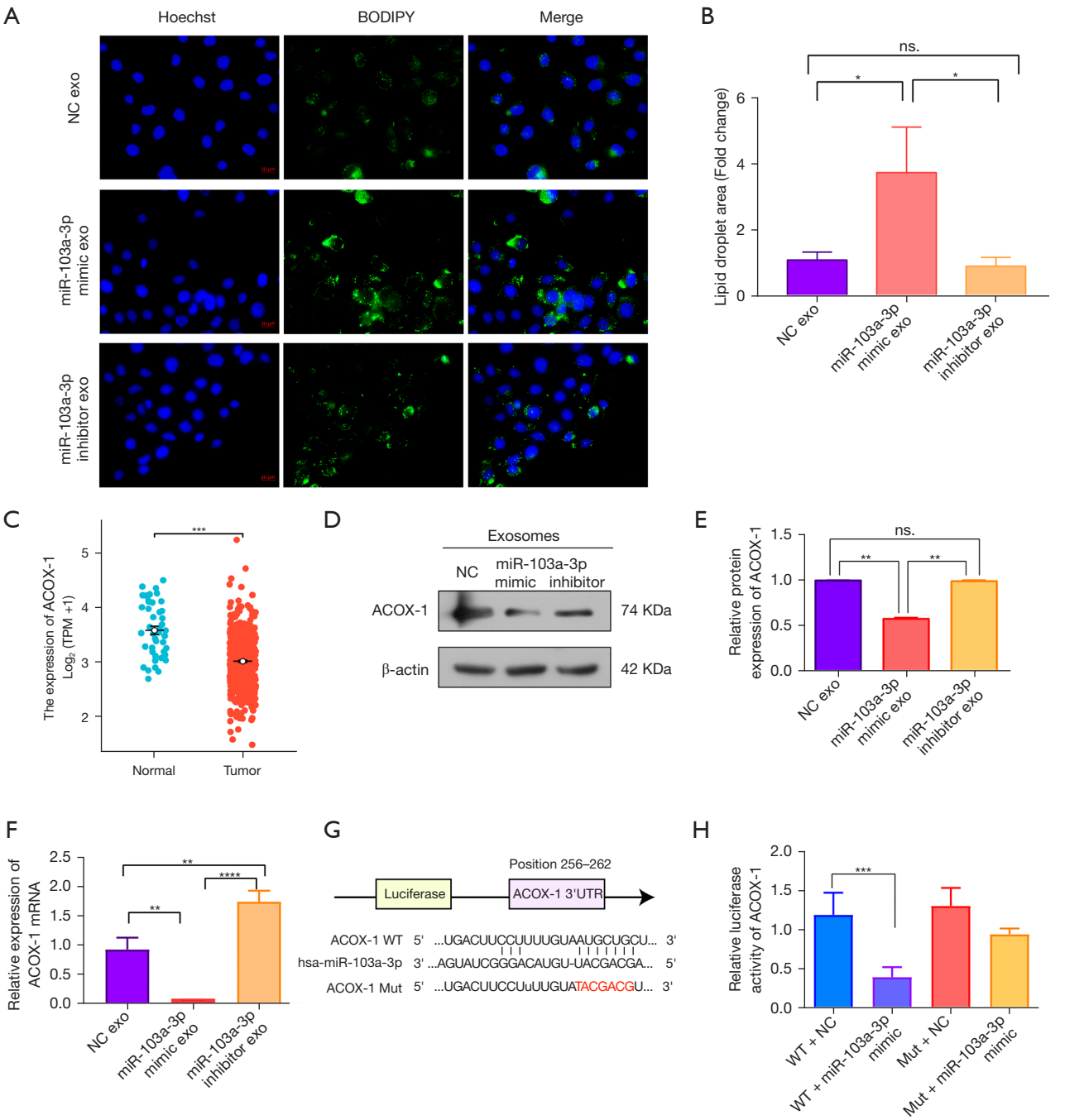

Figure 5 Exosomal miR-103a-3p causes abnormal lipid metabolism and enhances tumor growth by target ACOX-1 in nasopharyngeal carcinoma. (A) Representative immunofluorescent pictures of BODIPY 493/503 staining lipid droplets in exosomes treated CNE2 cells. Magnification: ×40. (B) Quantification of lipid droplet area. (C) Analysis of ACOX-1 expression in TCGA HNSC cohort. (D,E) ACOX-1 protein expression in exosomes co-cultured CNE2 cells. (F) Reverse transcription quantitative polymerase chain reaction (RT-qPCR) detected the ACOX-1 mRNA level in exosomes co-cultured CNE2 cells. (G) Scheme of the ACOX-1 3' UTR miR-103a-3p probable binding sites. (H) Luciferase activity of ACOX-13'UTR Wt or Mut plasmids in CNE2 cells after transfection with miR-103a-3p mimic or normal control (NC). Data represent at least three experiments performed in triplicate, ****, P<0.0001; ***, P<0.001; **, P<0.01; *, P<0.05; ns, non-significant. ACOX-1, acyl-CoA oxidase 1; mRNA, messenger RNA; TCGA, The Cancer Genome Atlas; HNSC, head and neck squamous cell carcinoma.

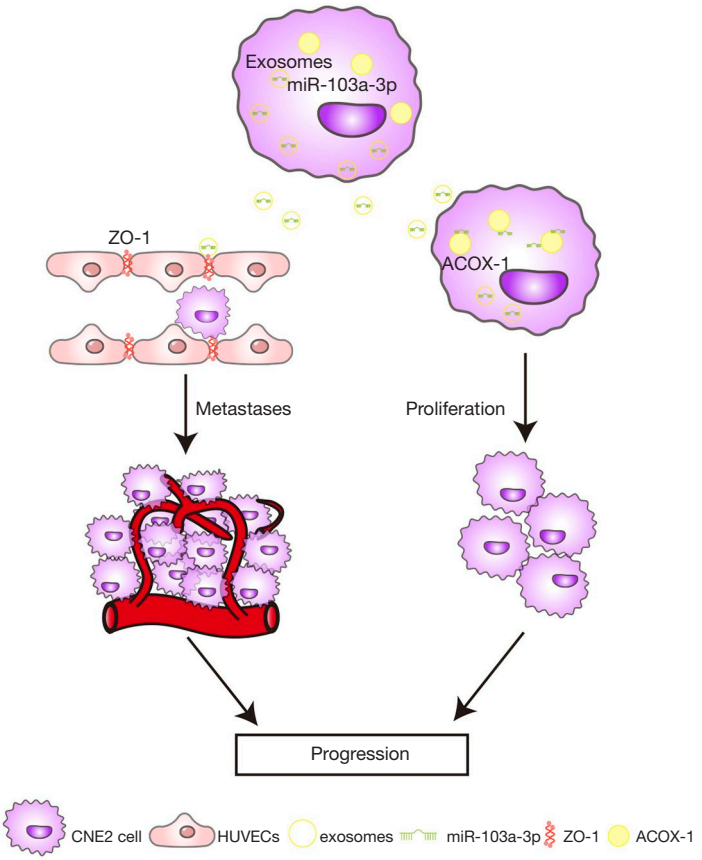

Figure 6 Schematic diagram illustrated Tumor-derived exosomal miR-103a-3p promotes vascular permeability and proliferation by targeting ZO-1 and ACOX-1 in nasopharyngeal carcinoma. HUVECs, human umbilical vein endothelial cells; ZO-1, zonula occludens 1; ACOX-1, acyl-CoA oxidase 1.

3p expression in comparison to the control group had a significant decline in ACOX-1 mRNA levels (*Figure 5F*). A region complementary to miR-103a-3p seed region was found in the 3' UTR of ACOX-1 as illustrated in *Figure 5G*. A dual-luciferase reporter system was applied to determine whether or not ACOX-1 was a direct target of miR-103a-3p using either the wild-type or mutant 3' UTR of ACOX-1. Co-transfection with the mutant ACOX-1 vector had no effect, whereas co-transfecting miR-103a-3p with wild-type ACOX-1 vector resulted in reduced luciferase activity (*Figure 5H*), indicating that miR-103a-3p bound the anticipated binding site in the 3' UTR of ACOX-1 directly and specifically.

These findings indicated that cancer-derived exosomal miR-103a-3p caused vascular leakiness and tumor proliferation, which in turn promotes NPC progression, as shown in *Figure 6*.

Discussion

NPC, a kind of epithelial cancer, has been demonstrated to develop in the nasopharynx (1). NPC has a significant potential for metastatic spread. The insidious nature of NPC's start and rapid growth and metastases makes diagnosis challenging (2). Clinical studies have shown that nearly all NPC patients in advanced stages have invasive growth at the base of the skull and that around 70% of patients with NPC develop metastasis to the neck lymph nodes (30-32). The molecular mechanisms behind NPC development, particularly the metastatic and proliferative processes, are still unknown. To develop innovative treatment strategies that are effective for NPC patients, a deeper comprehension of the molecular patterns of NPC metastasis and proliferation is needed. Clinical examination of the TCGA data revealed that miR-103a-3p expression

levels were elevated in NPC samples (*Figure 1A-1D*).

It is becoming more obvious that the tumor microenvironment (TME) is important for driving treatment resistance, metastasis, and tumor growth. The complex network of tumor-associated cells and noncellular elements that makes up the TME of NPC promotes the growth of tumors (33). Exosomes secreted by stromal cells as well as NPC cells are the key mediators of cell-to-cell communication in the TME, which facilitate NPC aggravation (34). They are regarded as one of the most important mechanisms for determining the various TME features (33). Exosomes have the potential to be useful biomarkers in NPC because they can alter the TME, take part in fast proliferation, promote pathological angiogenesis, and assist metastasis. They can also cause immune suppression and increase chemo- and radiation resistance (35).

As exosomes containing nucleic acid medicines have low immunogenicity and good biocompatibility, exosomes have entered the new industrial therapeutic frontiers as both drug delivery systems and intrinsic therapeutic agents (36). Because endogenous RNase prevents miRNAs from being degraded, miRNAs in exosomes are more stable. Exosomes containing miRNAs therefore hold significant promise for the clinical therapy of many types of cancer as NPC (37). Exosomes have been loaded with let-7a miRNA to target epidermal growth factor receptor (EGFR)-expressing xenograft breast cancer tissue and inhibit tumor development *in vivo* (36). AntagomiR-BART10-5p and antagomiR-18a, two iRGD-tagged exosomal antagomiRs, had a significant anti-angiogenesis and anti-tumor therapeutic impact on NPC when administered *in vivo* (38). Currently, more than 20 miRNA-based medicines are undergoing clinical trials. While no miRNA drug has been approved thus far, biotechnology companies such as Regulus Therapeutics, Synlogic, and Miragen are making progress toward developing miRNA-related drugs. The limited targeting ability of exosome-based tumor medication delivery systems severely limits their real applicability (39). Exosomes are still in their early stages of clinical application; more research will help identify time- and money-efficient nanotechnologies for exosome synthesis on a big scale (39).

Exosomes are prevalent in many bodily fluids, including breast milk, urine, saliva, blood, and amniotic fluid. As a result, exosomes can also be used as a non-invasive or minimally invasive method for the early identification of a variety of diseases. Furthermore, miRNAs packed to exosomes should be protected and more stable in bodily fluids than naked RNA, which is more likely to breakdown (36). Exosomes from patients with NPC have been found to have dysregulated miRNA expressions which control the expression of genes involved in cell division, differentiation, and stress response (36). It has been shown that exosomes released by NPC cells *in vivo* include loaded Epstein-Barr virus (EBV)-miR-BARTs that are stable enough to spread from tumor tissue into the peripheral circulation (36). As an oncomiR, miR-103a-3p has been previously reported overexpressed in exosomes of multiple cancers, including liver cancer, thyroid cancer, lung cancer, CRC, cervical cancer, glioblastoma (40). The levels of serum exosome-derived miR-103a-3p were significantly different among patients with multiple myeloma (MM) (41). Exosomal miR-103a-3p derived from cancer-associated fibroblast (CAF) promoted non-small cell lung cancer (NSCLC) cells cisplatin resistance by suppressing apoptosis (42). This study also discovered a sizable increase of miR-103a-3p in NPC tissues and exosomes generated from NPC cells (*Figure 1E-1F*). We then proposed that exosomal miR-103a-3p could be used as a prognostic marker and a potential therapeutic target.

Exosomes from cancer are sent into ordinary stromal cells in the target organ to promote metastasis or develop pre-metastatic niches. Then, we focused on the function of exosomal miR-103a-3p in NPC metastasis and growth, reasoning that miR-103a-3p could be contributing to malignant behavior via exosomes. Our findings showed that NPC cells exchanged miR-103a-3p through exosomes into the TME to promote the development of tumors. Exosomes were used to release miR-103a-3p into the extracellular space, and recipient HUVECs and cancer cells both took these exosomes up (*Figure 4D*) as well as the observed cancer cells. Notably, the miR-103a-3p enriched exosomes significantly sped up the cell-cycle transition (*Figure 3F-3H*), colony formation (*Figure 3B,3C*), proliferation (*Figure 3A,3D*), migration (*Figure 2E,2F,2H,2I*), and EMT progression (Figure S1A-S1C) in the recipient cancer cells. In contrast, after inhibiting the expression of miR-103a-3p, exosomes had no impact on the malignant activity of cancer cells. Cancer-induced vascular permeability is a crucial stage in the metastatic process (14). The cell-to-cell connections between endothelial cells consist of adhesion junctions and tight junctions, and they are crucial for maintaining vascular integrity (14). Through the destruction of the vascular barrier and subsequent changes in cancer cell migration to the stroma, the destruction of junction-associated proteins and tight junction aids in the spread of cancer (14). By using target prediction, we discovered that ZO-1 may function

as a directed target of miR-103a-3p (*Figure 4A*,*4M*,*4N*). Targets can also be regulated by many mechanisms. To support this idea, Western blot and RT-qPCR assay data found that miR-103a-3p overexpressed exosomes reduced ZO-1 expression at the protein (*Figure 4J*,*4K*) and mRNA (*Figure 4L*) levels. In line with this notion, our research showed that exosomal miR-103a-3p targeted ZO-1 in endothelial cells to establish the pre-metastatic niche to establish a favorable pre-metastatic niche in the stromal microenvironment (*Figure 4M*,*4N*).

There has long been interest in two key characteristics of tumors: metabolic reprogramming and invasive metastasis. Recent research has shown that these two malignant characteristics are intimately related rather than independent. Metabolic reprogramming of tumor cells is emerging as a critical feature of the TME influencing tumor growth, metastasis, and response to therapy (43). By sustaining proliferation, metabolic reprogramming influences tumor development and progression. Acyl-CoA is converted to enoyl-CoA by the metabolic enzyme ACOX-1, which is a rate-limiting enzyme in peroxisomal fatty acid -oxidation. ACOX-1 exhibits abnormally low expression in numerous malignancies, including lymphoma and bladder cancer (20,21). ACOX-1 is a metabolic enzyme that has been demonstrated to slow the growth of CRC by controlling the reprogramming of palmitic acid (PA), according to earlier research (22). These studies show that ACOX-1 inhibits cancer growth. In light of prior research that demonstrated ACOX-1 being involved in cancer cell proliferation, we might take into account the possibility that miR-103a-3p's targeting of ACOX-1 may affect NPC carcinogenesis and development (*Figure 4A*). This would advance our comprehension of how ACOX-1 promotes tumor growth. CCK8 (*Figure 3A*), colony formation (*Figure 3B*,*3C*), EdU (*Figure 3D*) and flow cytometry (*Figure 3F-3H*) assay data indicated that miRNA-103a-3p overexpressed exosomes accelerated the cell proliferation and promoted the lipid droplet accumulation (*Figure 5A*), which suggested that in contrast to the control (miR-NC) and miR-103a-3p inhibitor, miR-103a-3p mediates lipid metabolism to boost NPC cell proliferation. Furthermore, miR-103a-3p mimic-transfected exosomes treated CNE2 cells resulted in a downregulation of ACOX-1 expression at the protein (*Figure 5D*,*5E*) and mRNA (*Figure 5F*) levels, respectively. The 3'-UTR of ACOX-1 and miR-103a-3p directly bind, according to luciferase activity assays (*Figure 5G*,*5H*).

We identified that miR-103a-3p is a pro-metastatic miRNA in exosomes released by NPC cells and a negative regulator of two targets, ZO-1 and ACOX-1, in the current study. Although miR-103a-3p's regulatory involvement in NPC advancement has been mentioned previously, this is the first report demonstrating that miR-103a-3p is highly concentrated in NPC exosomes and directly regulate growth and metastasis by targeting ACOX-1 and ZO-1 in NPC. However, this study primarily focused on the intercellular contact between NPC cells and HUVECs and only provided *in vitro* evidence. Further research will be conducted in subsequent studies for specific molecular pathways behind the miR-103a-3p/ACOX-1 axle in lipid metabolism.

Conclusions

In this study, we observed that inhibiting miR-103a-3p suppressed proliferation and blocked the migration of NPC cells by targeting ZO-1 and ACOX-1. Our study elucidated a novel molecular mechanism of exosomes promoting NPC progression underlying the interaction between NPC cells and HUVECs.

Acknowledgments

Funding: This work was supported by Grants from the National Natural Science Foundation of China (grant Nos. 82103435, 82173288), construction unit of key medical discipline laboratory in Jiangsu province during the 14th Five Year Plan period.

Footnote

Reporting Checklist: The authors have completed the MDAR and ARRIVE reporting checklists. Available at https://tcr.amegroups.com/article/view/10.21037/tcr-23-2359/rc

Data Sharing Statement: Available at https://tcr.amegroups.com/article/view/10.21037/tcr-23-2359/dss

Peer Review File: Available at https://tcr.amegroups.com/article/view/10.21037/tcr-23-2359/prf

Conflicts of Interest: All authors have completed the ICMJE uniform disclosure form (available at https://tcr.amegroups.com/article/view/10.21037/tcr-23-2359/coif). The authors have no conflicts of interest to declare.

Ethical Statement: The authors are accountable for all

aspects of the work in ensuring that questions related to the accuracy or integrity of any part of the work are appropriately investigated and resolved. The study was conducted in accordance with the Declaration of Helsinki (as revised in 2013) and was approved by the ethics committee of the Affiliated Hospital of Nantong University (No. 2018-L052). Informed consent was taken from all the patients. Animal experiments were performed under a project license (No. 20180227-005) granted by the Institutional Animal Care and Research Advisory Committee of Nantong University and in compliance with institutional guidelines for the care and use of animals.

References

1. Huang H, Yao Y, Deng X, et al. Immunotherapy for nasopharyngeal carcinoma: Current status and prospects (Review). Int J Oncol 2023;63:97.
2. Campion NJ, Ally M, Jank BJ, et al. The molecular march of primary and recurrent nasopharyngeal carcinoma. Oncogene 2021;40:1757-74.
3. Yang Q, Wu F, Zhang Y, et al. FOXM1 regulates glycolysis in nasopharyngeal carcinoma cells through PDK1. J Cell Mol Med 2022;26:3783-96.
4. Zhang D, Huang H, Sun Y, et al. CircHIPK2 promotes proliferation of nasopharyngeal carcinoma by down-regulating HIPK2. Transl Cancer Res 2022;11:2348-58.
5. Navarro-Manzano E, Luengo-Gil G, González-Conejero R, et al. Prognostic and Predictive Effects of Tumor and Plasma miR-200c-3p in Locally Advanced and Metastatic Breast Cancer. Cancers (Basel) 2022;14:2390.
6. Chung J, Kim KH, Yu N, et al. Fluid Shear Stress Regulates the Landscape of microRNAs in Endothelial Cell-Derived Small Extracellular Vesicles and Modulates the Function of Endothelial Cells. Int J Mol Sci 2022;23:1314.
7. Yao J, Chen Y, Lin Z. Exosomes: Mediators in microenvironment of colorectal cancer. Int J Cancer 2023;153:904-17.
8. Shen D, He Z. Mesenchymal stem cell-derived exosomes regulate the polarization and inflammatory response of macrophages via miR-21-5p to promote repair after myocardial reperfusion injury. Ann Transl Med 2021;9:1323.
9. Liu K, Dou R, Yang C, et al. Exosome-transmitted miR-29a induces colorectal cancer metastasis by destroying the vascular endothelial barrier. Carcinogenesis 2023;44:356-67.
10. Gautam SK, Batra SK, Jain M. Molecular and metabolic regulation of immunosuppression in metastatic pancreatic ductal adenocarcinoma. Mol Cancer 2023;22:118.
11. Zhao F, Li Z, Dong Z, et al. Exploring the Potential of Exosome-Related LncRNA Pairs as Predictors for Immune Microenvironment, Survival Outcome, and Microbiotain Landscape in Esophageal Squamous Cell Carcinoma. Front Immunol 2022;13:918154.
12. Bao L, You B, Shi S, et al. Metastasis-associated miR-23a from nasopharyngeal carcinoma-derived exosomes mediates angiogenesis by repressing a novel target gene TSGA10. Oncogene 2018;37:2873-89.
13. Baqai U, Purwin TJ, Bechtel N, et al. Multi-omics Profiling Shows BAP1 Loss Is Associated with Upregulated Cell Adhesion Molecules in Uveal Melanoma. Mol Cancer Res 2022;20:1260-71.
14. Li K, Xue W, Lu Z, et al. Tumor-derived exosomal ADAM17 promotes pre-metastatic niche formation by enhancing vascular permeability in colorectal cancer. J Exp Clin Cancer Res 2024;43:59.
15. Wautier JL, Wautier MP. Vascular Permeability in Diseases. Int J Mol Sci 2022;23:3645.
16. Yokota Y, Noda T, Okumura Y, et al. Serum exosomal miR-638 is a prognostic marker of HCC via downregulation of VE-cadherin and ZO-1 of endothelial cells. Cancer Sci 2021;112:1275-88.
17. Dou R, Liu K, Yang C, et al. EMT-cancer cells-derived exosomal miR-27b-3p promotes circulating tumour cells-mediated metastasis by modulating vascular permeability in colorectal cancer. Clin Transl Med 2021;11:e595.
18. Onésime D, Vidal L, Thomas S, et al. A unique, newly discovered four-member protein family involved in extracellular fatty acid binding in Yarrowia lipolytica. Microb Cell Fact 2022;21:200.
19. Zheng R, Wang Y. SLC9A5 promotes tumor growth and cell motility via ACOX1-mediated peroxisomal fatty acid oxidation. Exp Cell Res 2023;430:113700.
20. Zheng FM, Chen WB, Qin T, et al. ACOX1 destabilizes p73 to suppress intrinsic apoptosis pathway and regulates

sensitivity to doxorubicin in lymphoma cells. BMB Rep 2019;52:566-71.
21. Zhang Q, Yang X, Wu J, et al. Reprogramming of palmitic acid induced by dephosphorylation of ACOX1 promotes β-catenin palmitoylation to drive colorectal cancer progression. Cell Discov 2023;9:26. Correction appears in Cell Discov 2023;9:35.
22. Huang J, Viswakarma N, Yu S, et al. Progressive endoplasmic reticulum stress contributes to hepatocarcinogenesis in fatty acyl-CoA oxidase 1-deficient mice. Am J Pathol 2011;179:703-13.
23. Lai YH, Liu H, Chiang WF, et al. MiR-31-5p-ACOX1 Axis Enhances Tumorigenic Fitness in Oral Squamous Cell Carcinoma Via the Promigratory Prostaglandin E2. Theranostics 2018;8:486-504.
24. Xie L, Zhang K, You B, et al. Hypoxic nasopharyngeal carcinoma-derived exosomal miR-455 increases vascular permeability by targeting ZO-1 to promote metastasis. Mol Carcinog 2023;62:803-19.
25. Zhao Y, Gu X, Wang Y. MicroRNA-103 promotes nasopharyngeal carcinoma through targeting TIMP-3 and the Wnt/β-catenin pathway. Laryngoscope 2020;130:E75-E82.
26. Wang M, Shu H, Cheng X, et al. Exosome as a crucial communicator between tumor microenvironment and gastric cancer (Review). Int J Oncol 2024;64:28.
27. Shu L, Li X, Liu Z, et al. Bile exosomal miR-182/183-5p increases cholangiocarcinoma stemness and progression by targeting HPGD and increasing PGE2 generation. Hepatology 2024;79:307-22.
28. Ang HL, Mohan CD, Shanmugam MK, et al. Mechanism of epithelial-mesenchymal transition in cancer and its regulation by natural compounds. Med Res Rev 2023;43:1141-200.
29. Safi R, Menéndez P, Pol A. Lipid droplets provide metabolic flexibility for cancer progression. FEBS Lett 2024;598:1301-27.
30. Mo Y, Wang Y, Zhang S, et al. Circular RNA circRNF13 inhibits proliferation and metastasis of nasopharyngeal carcinoma via SUMO2. Mol Cancer 2021;20:112.
31. Jiang D, Li Y, Cao J, et al. Cell Division Cycle-Associated Genes Are Potential Immune Regulators in Nasopharyngeal Carcinoma. Front Oncol 2022;12:779175.
32. Du M, Hu X, Jiang X, et al. LncRNA EPB41L4A-AS2 represses Nasopharyngeal Carcinoma Metastasis by binding to YBX1 in the Nucleus and Sponging MiR-107 in the Cytoplasm. Int J Biol Sci 2021;17:1963-78.
33. Liu H, Tang L, Li Y, et al. Nasopharyngeal carcinoma: current views on the tumor microenvironment's impact on drug resistance and clinical outcomes. Mol Cancer 2024;23:20.
34. Luo H, Yi B. The role of Exosomes in the Pathogenesis of Nasopharyngeal Carcinoma and the involved Clinical Application. Int J Biol Sci 2021;17:2147-56.
35. Liu Y, Wen J, Huang W. Exosomes in nasopharyngeal carcinoma. Clin Chim Acta 2021;523:355-64.
36. Liao C, Liu H, Luo X. The emerging roles of exosomal miRNAs in nasopharyngeal carcinoma. Am J Cancer Res 2021;11:2508-20.
37. Nam GH, Choi Y, Kim GB, et al. Emerging Prospects of Exosomes for Cancer Treatment: From Conventional Therapy to Immunotherapy. Adv Mater 2020;32:e2002440.
38. Wang J, Jiang Q, Faleti OD, et al. Exosomal Delivery of AntagomiRs Targeting Viral and Cellular MicroRNAs Synergistically Inhibits Cancer Angiogenesis. Mol Ther Nucleic Acids 2020. [Epub ahead of print]. doi: 10.1016/j.omtn.2020.08.017.
39. Yang M, Wang X, Pu F, et al. Engineered Exosomes-Based Photothermal Therapy with MRI/CT Imaging Guidance Enhances Anticancer Efficacy through Deep Tumor Nucleus Penetration. Pharmaceutics 2021;13:1593.
40. Li L, Qiu A, Shi Y. MiR-103a-3p Promotes Tumorigenesis of Breast Cancer by Targeting ETNK1. Iran J Public Health 2024;53:208-18.
41. Zhang ZY, Li YC, Geng CY, et al. Serum exosomal microRNAs as novel biomarkers for multiple myeloma. Hematol Oncol 2019;37:409-17.
42. Wang H, Huang H, Wang L, et al. Cancer-associated fibroblasts secreted miR-103a-3p suppresses apoptosis and promotes cisplatin resistance in non-small cell lung cancer. Aging (Albany NY) 2021;13:14456-68.
43. Zheng Y, Wu R, Wang X, et al. Identification of a Four-Gene Metabolic Signature to Evaluate the Prognosis of Colon Adenocarcinoma Patients. Front Public Health 2022;10:860381.

Cite this article as: Shan Y, Fan H, Chai L, Kong X, Xiao H, You M, You Y. Tumor-derived exosomal miR-103a-3p promotes vascular permeability and proliferation by targeting ZO-1 and ACOX-1 in nasopharyngeal carcinoma. Transl Cancer Res 2024;13(9):4896-4912. doi: 10.21037/tcr-23-2359

